

Role of Halide Ion in the Mechanism of Protonolysis of the Pt–C Bond in Pt(II) Alkyl and Aryl Complexes

G. ALIBRANDI, D. MINNITI, R. ROMEO

Department of Chemistry, University of Messina, Italy

P. UGUAGLIATI

Centro Chimica Tecnologia Composti Metallorganici Elementi di Transizione C.N.R., Istituto Chimica Industriale, University of Padua, Italy

L. CALLIGARO, U. BELLUCO

Cattedre di Chimica, Faculty of Engineering, University of Padua, Italy

and B. CROCIANI

Istituto di Chimica Generale, University of Palermo, Italy

Received November 26, 1984

Abstract

A mechanistic study is described for the electrophilic cleavage of the Pt–C σ bond in complexes *cis*-[PtPh₂(PEtPh₂)₂] and *trans*-[PtXR(PEt₃)₂] (X = Cl and Br, R = Me, Et, n-Pr, n-Bu, CH₂Ph) by the proton in the presence of halide ions in aqueous methanol (MeOH/H₂O, 9/1 v/v) which yields *cis*-[PtClPh(PEtPh₂)₂] and *trans*-[PtX₂(PEt₃)₂], respectively. The reactions are first-order in substrate for both systems and the general bivariate rate law $k_{\text{obs}} = [\text{H}^+]\{k_{\text{H}} + k_{\text{X}}K[\text{X}^-]\}/(1 + K[\text{X}^-])$ is obeyed. The proposed mechanism involves a fast pre-equilibrium formation (K) of a platinum(II) anionic intermediate via interaction of the halide with the square-planar substrate, combined with slow, parallel protonation of both the substrate (k_{H}) and the intermediate (k_{X}), causing the cleavage of the metal–carbon σ bond. The intermediate should be conceived of as a weak association product, since all attempts at measuring the constant K by UV, visible and ³¹P{¹H} NMR spectroscopy were unsuccessful. This mechanism will rationalize the previously reported diverse kinetic results for the protonolysis of Pt–C σ bonds, within a unified picture which takes into account the electronic and steric properties of the group to be cleaved and of ancillary ligands. The role of the halide ion can be put into evidence by the use of substrates that will promote association through a reduced electron density on the central metal.

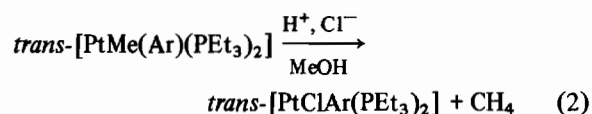
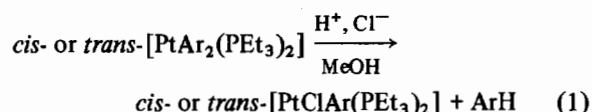
Introduction

The mechanism of electrophilic cleavage of metal–carbon bonds in transition metal complexes has been

thoroughly investigated for a variety of substrates, as described in recent reviews [1, 2]. The reactivity patterns have been interpreted in terms of either direct attack on the M–C σ bond, attack on the aromatic ring in the case of metal aryl substrates, or prior oxidative addition to the central metal followed by reductive elimination.

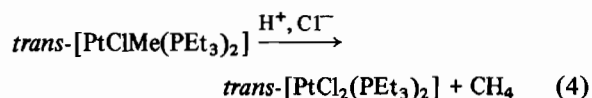
In the case of the protonolysis of alkyl- and aryl Pt(II) tertiary phosphine complexes by hydrochloric acid in methanol, different dependencies of rate on proton and halide concentrations have been observed.

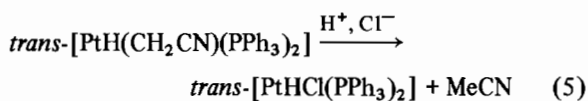
For bis-aryl substrates of type *cis*- or *trans*-[PtAr₂(PEt₃)₂] (Ar = aryl group), and mixed methyl–aryl derivatives *trans*-[PtMe(Ar)(PEt₃)₂], the pseudo-first order rate constant k_{obs} was linearly dependent on proton concentration [3–5] but independent of chloride concentration:



$$k_{\text{obs}} = k_2[\text{H}^+] \quad (3)$$

The protonolysis of monoalkylplatinum(II) derivatives [6, 7] (eqns. 4, 5):





was found to follow a two-term rate law with both proton and chloride linear dependence:

$$k_{\text{obs}} = k_2 [\text{H}^+] + k_3 [\text{H}^+][\text{Cl}^-] \quad (6)$$

For the systems obeying rate law (3), a mechanism has been proposed which involves a direct rate-determining attack of the proton on the Pt–C bond with release of ArH in a three-center transition state. For the systems obeying rate law (6), a fast protonation preequilibrium was proposed leading to a Pt(IV) labile hydrido species via oxidative addition, followed by slow reductive elimination of alkane both in a monomolecular step and in a bimolecular, chloride-promoted path. A study of the electrophilic cleavage of metal–carbon σ bonds in mixed alkyl–aryl transition metal complexes of general formula [MRArL_n] was purported to show that an S_E mechanism would explain the selective cleavage of the metal–aryl bond in *cis*-[AuMe₂Ph(PPh₃)] and [PtMe(4-MeC₆H₄)(C₈H₁₂)], whereas an oxidative-addition–reductive-elimination process would lead to selective cleavage of metal–methyl bond, as in *cis*-[PtMePh(PMePh₂)₂] [8].

These manifold results suggested that the particular mechanism observed appeared to depend on several factors, such as the electronic and steric properties of the group to be cleaved and of ancillary ligands, the steric configuration of the substrate and the solvating ability of the medium.

In an effort to lay down a general mechanism for protonolysis which would rationalize the previously reported kinetic results (in particular, the diverse chloride ion dependence) within a unified picture, we have followed a novel approach centered on the preequilibrium formation of a key ‘five-coordinate’ anionic intermediate upon interaction of chloride with the square-planar substrate, combined with slow *parallel* protonation of both the substrate and the intermediate [2]. We sought experimental evidence for such a mechanism by choosing platinum(II) substrates with ancillary ligands of reduced electron donor properties in order to promote the initial formation of the chloride intermediate adduct owing to a decreased electron density on the central metal. This aim was achieved with the systems *cis*-[PtPh₂(PEtPh₂)₂] and *trans*-[PtXR(PEt₃)₂], as will be described.

Experimental

Materials

Anhydrous methanol was obtained by distillation of the reagent grade solvent over Mg(OMe)₂. LiClO₄

‘anhydrous’ (99.8%) was purchased from K and K Fine and Rare Chemicals. All other reagents were used without further purification.

Preparation of Platinum(II) Substrates

The complexes *trans*-[PtXR(PEt₃)₂] (X = Cl and Br, R = Me; X = Cl, R = Et, CH₂Ph) were prepared by literature methods [9]. The complex *trans*-[PtCl(n-Pr)(PEt₃)₂] was prepared by *cis*–*trans* isomerization promoted by free PEt₃ from the corresponding *cis* isomer, as follows: the compound *cis*-[PtCl(n-Pr)(PEt₃)₂] (0.20 g) was suspended in light petroleum (10 ml) and PEt₃ (0.04 ml) was added under N₂. Upon heating to reflux, a clear solution was obtained, which was cooled to room temperature and evaporated to dryness under vacuum to give a colourless residue. This was recrystallized from light petroleum at –20 °C to yield the *trans* isomer as colourless prisms (0.17 g; m.p. 49–50 °C). *Anal.* Calcd. for C₁₅H₃₇ClP₂Pt: C, 35.33; H, 7.31. Found: C, 35.6; H, 7.4%. ³¹P{¹H} NMR in C₆D₆: δ /ppm, 15.2 downfield from external 85% H₃PO₄; ¹J(Pt–P), 2959 Hz.

The homologue *trans*-[PtCl(n-Bu)(PEt₃)₂] was prepared in a similar way. *Anal.* Calcd. for C₁₆H₃₉ClP₂Pt: C, 36.67; H, 7.50. Found: C, 36.4; H, 7.2%. ³¹P{¹H} NMR in C₆D₆: δ /ppm, 15.0; ¹J(Pt–P), 2961 Hz.

The complex *cis*-[PtPh₂(PEtPh₂)₂] was prepared by the ligand displacement reaction of [PtPh₂(COD)] (COD = η^4 -1,5-cyclooctadiene) with two equivalents of PEtPh₂ [10]. *Anal.* Calcd. for C₄₀H₄₀P₂Pt: C, 61.77; H, 5.18. Found: C, 61.6; H, 5.1%. ³¹P{¹H} NMR in CH₂Cl₂: δ /ppm, 16.2; ¹J(Pt–P), 1782 Hz.

Characterization of Protonolysis Products

The products from protonolysis reactions were identified by comparison of the final spectra after completion of kinetic runs with those of the corresponding authentic samples *trans*-[PtX₂(PEt₃)₂] (X = Cl, Br) and *cis*-[PtClPh(PEtPh₂)₂], respectively, which had been prepared independently. The latter compound was obtained by cleavage of one Pt–Ph bond in *cis*-[PtPh₂(PEtPh₂)₂] by hydrogen chloride [9]. *Anal.* Calcd. for C₃₄H₃₅ClP₂Pt: C, 55.39; H, 4.92; Cl, 4.81. Found: C, 55.2; H, 4.8; Cl, 4.9%. ν (Pt–Cl), 309 cm^{–1}. ³¹P{¹H} NMR in CH₂Cl₂: δ /ppm, 121.0 [¹J(Pt–P), 1630 Hz]; 115.7 [¹J(Pt–P), 4365 Hz]; ²J(P–P), 14.9 Hz.

Kinetics

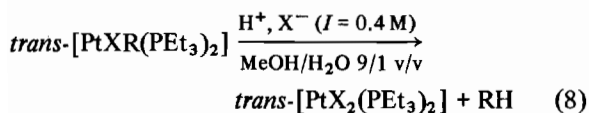
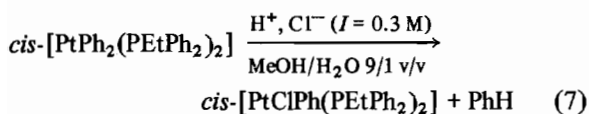
The kinetics were followed spectrophotometrically in MeOH/H₂O (9/1, v/v) under pseudo-first-order conditions at a constant ionic strength of 0.3–0.4 M (LiClO₄). The desired proton and chloride concentrations were obtained by transferring into a standard volumetric flask the appropriate amounts of standardized solutions of HClO₄, LiCl and LiClO₄. The

reactions were carried out in a silica cell in the thermostatted cell compartment of a double-beam Optica CF 4 or a Cary 219 spectrophotometer, with a temperature constant of ± 0.05 °C.

The reagent solution was brought to reaction temperature in the spectrophotometer and the reaction was started by adding an appropriate amount of a finely-powdered sample of the complex and shaking the solution rapidly. The spectra of the reacting systems were scanned from time to time between 320–220 nm. The pseudo-first-order rate constants k_{obs} were obtained from a non-linear least-squares fit of experimental data to $A_t = A_\infty + (A_0 - A_\infty)\exp(-k_{\text{obs}}t)$ with A_0 , A_∞ , and k_{obs} as the parameters to be optimized (A_0 = absorbance after mixing of reactants, A_∞ = absorbance at completion of reaction). This procedure proved especially useful for the slowest reactions, for which experimental observation of A_∞ was not feasible. Under the experimental conditions described, the protonolysis of *cis*-[PtPh₂(PEtPh₂)₂] involves the cleavage of only one Pt–Ph bond. The rates of cleavage of the remaining Pt–Ph bond in the product *cis*-[PtPhCl(PEtPh₂)₂] were too low to be measured. The rate parameters k_{H} , k_{Cl} , and K were obtained by multiple non-linear regression of k_{obs} vs. $[\text{H}^+]$ and $[\text{Cl}^-]$ dependencies. Activation parameters were derived from non-linear fits of k/T vs. T data according to the Eyring formalism. All statistical and graphical analyses of kinetic data were carried out on a Tektronix 4052 Graphic System (64 K RAM), with a 4662 Digital Plotter and a 4907 Floppy Disk Unit (1.8 MB).

Results and Discussion

The cleavage of Pt–C σ bonds by protonolysis takes place according to the following reactions:



(R = Me, Et, n-Pr, n-Bu, CH₂Ph; X = Cl)

(R = Me; X = Br)

Figure 1 shows the spectral changes observed with time for reaction (8) with R = Me, X = Cl. The pseudo-first-order rate constants, k_{obs} , for reaction (7) are listed in Table I for a range of H⁺ and Cl[−] concentrations at 40 °C. An analogous table of rate data for the system of reaction (8) has been deposited

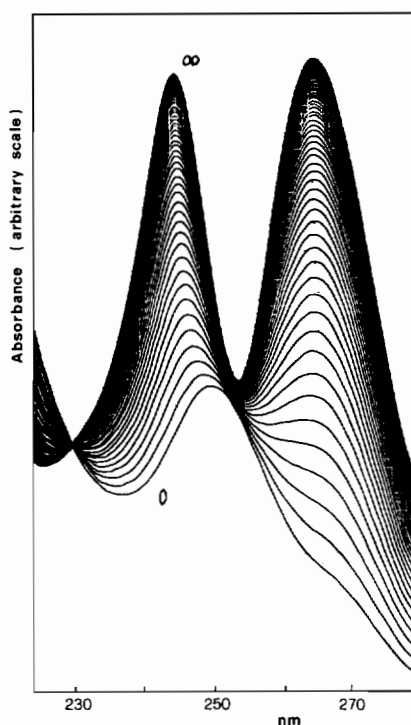


Fig. 1. Changes in optical density with time for the reaction $\text{trans-}[\text{PtClMe}(\text{PEt}_3)_2] \xrightarrow{\text{H}^+, \text{Cl}^-} \text{trans-}[\text{PtCl}_2(\text{PEt}_3)_2] + \text{CH}_4$ at 30 °C.

TABLE I. Rate Parameters for the Reaction $\text{cis-}[\text{PtPh}_2(\text{PEtPh}_2)_2] + \text{H}^+ + \text{Cl}^- \rightarrow \text{cis-}[\text{PtClPh}(\text{PEtPh}_2)_2] + \text{C}_6\text{H}_6$ in 9/1 v/v MeOH/H₂O at 40 °C. $I = 0.3 \text{ M}$ (LiClO₄).

[Cl [−]] M	10 ² [H ⁺] M	10 ⁴ k_{obs} s ^{−1}	[Cl [−]] M	10 ² [H ⁺] M	10 ⁴ k_{obs} s ^{−1}
0	1.30	0.54	0.13	3.80	6.23
0	2.52	0.91	0.13	5.04	7.88
0	3.80	1.58	0.13	6.30	10.33
0	5.04	1.92	0.13	7.56	12.53
0	6.30	2.63	0.20	1.30	2.47
0	7.56	3.35	0.20	2.52	4.81
0.04	1.30	1.29	0.20	3.80	7.22
0.04	2.52	2.37	0.20	5.04	9.20
0.04	3.80	3.78	0.20	6.30	11.97
0.04	5.04	4.73	0.20	7.56	14.60
0.04	6.30	6.27			
0.04	7.56	7.56			
0.06	1.30	1.55			
0.06	3.80	4.53			
0.06	5.04	5.67			
0.06	6.30	7.52			
0.06	7.56	9.20			
0.09	1.30	1.83			
0.09	2.52	3.57			
0.09	3.80	5.40			
0.09	5.04	7.08			
0.09	6.30	8.95			

(continued overleaf)

TABLE I (continued)

$[\text{Cl}^-]$ M	$10^2[\text{H}^+]$ M	$10^4 k_{\text{obs}}$ s^{-1}	$[\text{Cl}^-]$ M	$10^2[\text{H}^+]$ M	$10^4 k_{\text{obs}}$ s^{-1}
0.09	7.56	11.00			
0.13	1.30	2.13			
0.13	2.52	4.18			

with the Editor as Supplementary Material, and will be available upon request. The k_{obs} values appear to be a linear function of $[\text{H}^+]$ at constant $[\text{Cl}^-]$ with statistically non-significant intercept, whereas at constant $[\text{H}^+]$ a curvilinear dependence on $[\text{Cl}^-]$ is observed which levels off to a limiting value at high chloride concentration. We explain the observations in terms of formal H^+ and Cl^- concentration, since in the ranges examined we can expect the kinetics to reflect exactly the concentration changes despite any ion pair association. These dependencies are represented graphically in Figs. 2 and 3 for protonolysis of *trans*-[PtClMe(PET₃)₂] at 30 °C. A global 3-D representation is given in Fig. 4 for the kinetic data of protonolysis of *cis*-[PtPh₂(PEtPh₂)₂] at 40 °C. All the rate data appear to fit the bivariate non-linear rate law (9):

$$k_{\text{obs}} = [\text{H}^+] \cdot \frac{k_{\text{H}} + k_{\text{Cl}}K[\text{Cl}^-]}{1 + K[\text{Cl}^-]} \quad (9)$$

Table II lists the dependence of k_{obs} on $[\text{Cl}^-]$ at $[\text{H}^+] = 7.56 \times 10^{-2}$ M for reaction (7) at various temperatures, along with the k_{H} , k_{Cl} and K parameters obtained by non-linear bivariate regression analysis according to eqn. 9.

Non-linear regression analysis of k_{H} , k_{Cl} and K data vs. absolute temperature gives the following activation and thermodynamic parameters:

$$\begin{aligned} \Delta H_{\text{H}}^\ddagger &= 19.3 \pm 0.5 \text{ kcal/mol} & \Delta S_{\text{H}}^\ddagger &= -8 \pm 1 \text{ e.u.} \\ \Delta H_{\text{Cl}}^\ddagger &= 11.9 \pm 0.9 \text{ kcal/mol} & \Delta S_{\text{Cl}}^\ddagger &= -28 \pm 3 \text{ e.u.} \\ \Delta H^\circ &= 11 \pm 3 \text{ kcal/mol} & \Delta S^\circ &= 38 \pm 10 \text{ e.u.} \end{aligned}$$

In Table III are reported the corresponding rate parameters for reaction (8) at 30 °C.

All this evidence can be accommodated by a step-wise mechanism involving a fast pre-equilibrium formation of a platinum(II) anionic intermediate via interaction of the halide with the square-planar substrate, combined with slow, parallel protonation of both the substrate and the intermediate causing the cleavage of the metal-carbon σ bond (Scheme 1).

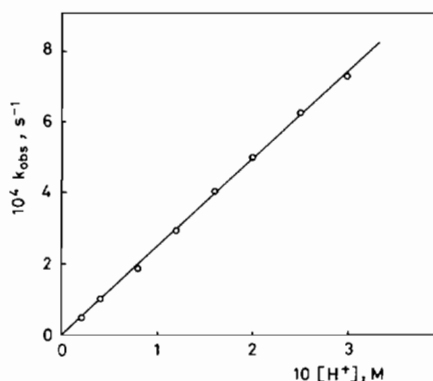


Fig. 2. Plot of k_{obs} vs. $[\text{H}^+]$ at $[\text{Cl}^-] = 0.1$ M for the protonolysis of *trans*-[PtClMe(PET₃)₂] at 30 °C.

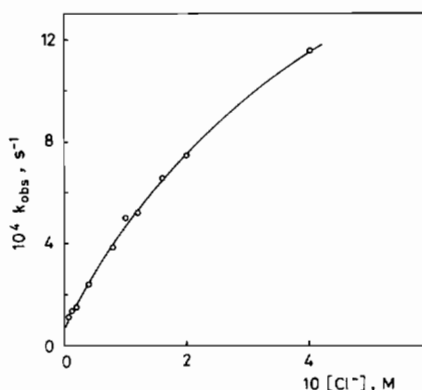


Fig. 3. Plot of k_{obs} vs. $[\text{Cl}^-]$ at $[\text{H}^+] = 0.2$ M for the protonolysis of *trans*-[PtClMe(PET₃)₂] at 30 °C.

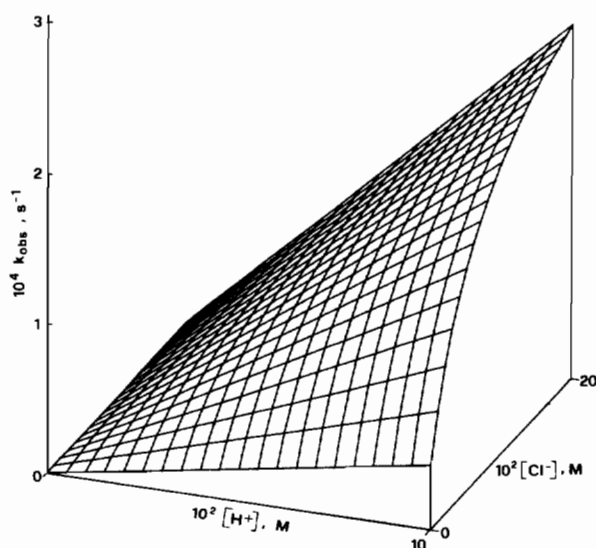


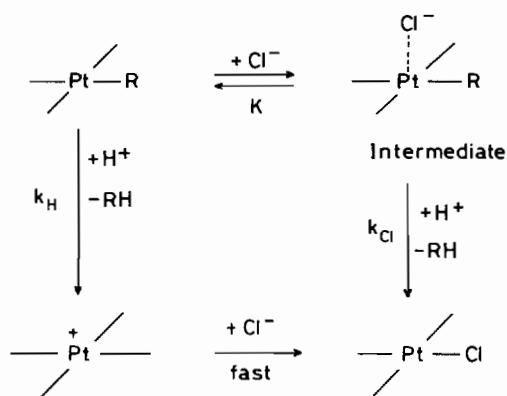
Fig. 4. 3-D representation of the dependence of k_{obs} on $[\text{H}^+]$ and $[\text{Cl}^-]$ for the protonolysis of *cis*-[PtPh₂(PEtPh₂)₂] at 40 °C.

TABLE II. Rate Parameters for the Reaction $cis\text{-[PtPh}_2\text{(PEtPh}_2\text{)}_2] + \text{H}^+ + \text{Cl}^- \rightarrow cis\text{-[PtClPh(PEtPh}_2\text{)}_2] + \text{C}_6\text{H}_6$ in 9/1 v/v MeOH/H₂O at Various Temperatures and at Constant Proton Concentration $[\text{H}^+] = 7.56 \times 10^{-2} \text{ M}$; $I = 0.3 \text{ M}$ (LiClO₄).

[Cl ⁻], M	$10^4 k_{\text{obs}}, \text{s}^{-1}$			
	20 °C	30 °C	35 °C	40 °C
0	0.40	1.16	1.91	3.35
0.03	0.67	2.28	4.17	7.00
0.06	0.94	3.25	5.68	9.20
0.09	1.09	3.73	6.71	11.00
0.12	1.37	4.52	7.52	12.25
0.16	1.60	5.03	8.53	13.60
0.20	1.81	5.63	9.20	14.60
$10^3 k_{\text{H}}, \text{M}^{-1} \text{s}^{-1}$	0.5 ± 0.1	1.6 ± 0.1	2.6 ± 0.1	4.4 ± 0.1
$10^2 k_{\text{Cl}}, \text{M}^{-1} \text{s}^{-1}$	0.8 ± 0.1	1.4 ± 0.1	1.87 ± 0.04	2.78 ± 0.06
K, M^{-1}	1.6 ± 0.5	4.5 ± 0.8	7.2 ± 0.5	8.8 ± 0.5

TABLE III. Rate Parameters for the Reactions $trans\text{-[PtXR(PEt}_3\text{)}_2] + \text{H}^+ + \text{X}^- \rightarrow trans\text{-[PtX}_2\text{(PEt}_3\text{)}_2] + \text{RH}$ in 9/1 v/v MeOH/H₂O at 30 °C. $I = 0.4 \text{ M}$ (LiClO₄).

X	R	$10^3 k_{\text{H}}$ ($\text{M}^{-1} \text{s}^{-1}$)	$10^2 k_{\text{X}}$ ($\text{M}^{-1} \text{s}^{-1}$)	K (M^{-1})
Cl	Me	0.38 ± 0.05	1.28 ± 0.1	1.97 ± 0.2
Br	Me	1.9 ± 1.9	56 ± 5	1.7 ± 0.2
Cl	Et	11.3 ± 0.4	9.1 ± 0.3	2.8 ± 0.2
Cl	n-Pr	8.2 ± 0.3	6.5 ± 0.3	2.6 ± 0.2
Cl	n-Bu	6.9 ± 0.5	4.9 ± 0.2	4.5 ± 0.5
Cl	Benzyl	0.24 ± 0.04	0.11 ± 0.01	5 ± 2



Scheme 1.

The preequilibrium constants (K) in Tables II and III appear to have high values, indicating that substantial formation of the intermediate takes place. However, attempts at detecting its presence by UV, visible and ³¹P NMR spectroscopy under conditions comparable to those of the kinetic studies were unsuccessful. Furthermore, abstract factor analysis of spectral changes during kinetic runs always showed the

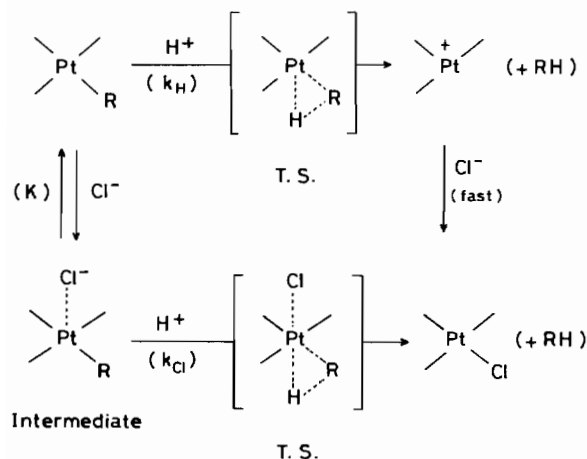
presence of only two independently-absorbing species (*i.e.*, the substrate and the final product) in the reaction mixtures [11]. This seems to indicate that the interaction between halide and substrate, while being kinetically important, is rather weak in nature and does not lead to a fully-fledged five-coordinate adduct, so that the spectral properties of the intermediate are virtually superimposable to those of the square-planar substrate*. On the other hand, a quite different mechanistic approach based on the steady-state approximation for the formation of the intermediate which would imply a very low, undetectable concentration for such a species, would yield a kinetic rate law in contrast with the observed H⁺ and Cl⁻ dependencies. The thermodynamic parameters suggest that formation of the intermediate is promoted by the positive standard entropy, mainly related to desolvation effects of the halide in the highly polar medium, which more than compensates for the endothermic nature of the process.

The k_{H} term in rate law (9) represents the electrophilic attack of the proton on the substrate, for which we propose the same mechanism as for related systems such as $cis\text{-[PtAr}_2\text{(PEt}_3\text{)}_2]$ [4]. The k_{Cl} term corresponds to an electrophilic attack on the anionic intermediate, for which an oxidative addition pathway also might be invoked [1–3, 6, 7, 12, 13]. This mechanistic picture is further supported by the higher values of k_{Cl} over k_{H} (*ca.* one order of magnitude) and by the activation parameters of reaction (7). The higher reactivity of the intermediate stems probably from a higher electron density at the reaction site, as reflected by the

*We surmise that the situation might be depicted as a weak apical interaction of chloride, outside the first coordination sphere and without substantial change in the substrate geometry.

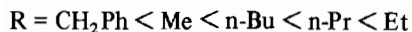
lower activation enthalpy for the k_{Cl} path. Consistently, the k_{X} term increases much more markedly than the k_{H} one on going from $\text{X} = \text{Cl}$ to $\text{X} = \text{Br}$ in the protonolysis of $\text{trans-}[\text{PtXMe}(\text{PEt}_3)_2]$ with HX (Table III).

The more negative entropy of activation of the k_{Cl} path is in accord with the proton attack on the intermediate being more restricted and strongly oriented by the presence of the chloride ion, which hinders a possible approach of the electrophile (apart from solvation effects, as shown in Scheme 2):



Scheme 2.

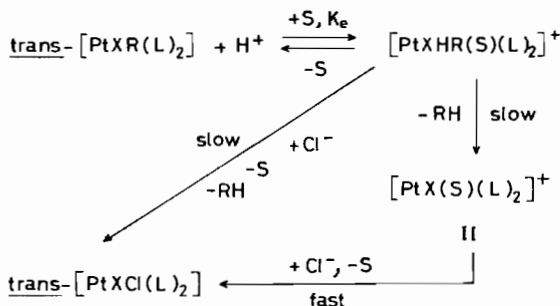
In the system $\text{trans-}[\text{PtClR}(\text{PEt}_3)_2]$, the k_{H} and k_{Cl} rate constants depend on the nature of R in the order



due to an interplay of electronic and steric factors. Replacement of a methyl hydrogen in $\text{trans-}[\text{PtClMe}(\text{PEt}_3)_2]$ by an electron-donating alkyl group brings about an increase in both k_{H} and k_{Cl} terms, with steric bulkiness playing an adverse role with increasing length of the alkyl chain. An increased protonolysis rate with increasing electron density and decreasing steric requirements at the protonation site has previously been observed for the cleavage of substituted phenyl derivatives $\text{cis-}[\text{Pt}(\text{C}_6\text{H}_4\text{Y})_2(\text{PEt}_3)_2]$ [4] and for the cleavage of the Pt-Me bond in $\text{trans-}[\text{PtMe}(\text{Ar})(\text{PEt}_3)_2]$ [5]. Consistently, the complex $\text{trans-}[\text{PtCl}(\text{CH}_2\text{-Ph})(\text{PEt}_3)_2]$ exhibits the lowest reactivity owing to the electron-withdrawing ability and size of the phenyl group. In contrast with the above kinetic effects, the pre-equilibrium constant K appears to be scarcely affected by R .

The bivariate rate law (9) can accommodate all previous mechanistic patterns observed for the protonolysis of Pt-C σ bonds, with the pre-equilibrium constant K being the discriminating factor

that dictates the particular form of the observed rate expression. In fact, when K is exceedingly low (*i.e.*, when no kinetically appreciable formation of the halide intermediate takes place), eqn. 9 reduces to the simple expression $k_{\text{obs}} = k_{\text{H}}[\text{H}^+]$, as found in the protonolysis of trans- and $\text{cis-}[\text{PtAr}_2(\text{PEt}_3)_2]$ and $\text{trans-}[\text{PtMe}(\text{Ar})(\text{PEt}_3)_2]$ [3–5]. When the K value increases, an intermediate situation will hold wherein the $K[\text{Cl}^-]$ term will be $\ll 1$, so that a two-term linear rate law $k_{\text{obs}} = k_{\text{H}}[\text{H}^+] + k_{\text{Cl}}K[\text{Cl}^-][\text{H}^+]$ is obtained. A similar linear dependence was found experimentally for the system $\text{trans-}[\text{PtH}(\text{CH}_2\text{-CN})(\text{PPh}_3)_2]$ [7]. This rate law was then interpreted in terms of an alternative mechanism involving prior reversible protonation of the substrate followed by reductive elimination of MeCN , which can take place both intramolecularly (chloride-independent path) and under the influence of an entering chloride ion (Scheme 3):



Scheme 3.

However, in the light of the present results, we suggest that the mechanism for this system is better rationalized by the general pattern of Scheme 1.

An analogous linear rate law was also proposed for the protonolysis of $\text{trans-}[\text{PtClMe}(\text{PEt}_3)_2]$ [6], but this appears to be an artifact of the very narrow range of Cl^- concentrations explored in that study. Re-examination of this system in the present work (Table III) has clearly shown that the kinetic data fit well into eqn. 9 (Fig. 3).

From the body of evidence gathered so far for these reactions, it appears that the pre-equilibrium constant K increases with decreasing electron-donating ability of the ancillary ligands in the platinum(II) substrate, under comparable steric conditions. The situation is illustrated by the different behaviour of the complexes $\text{cis-}[\text{PtPh}_2(\text{PEt}_3)_2]$ and $\text{cis-}[\text{PtPh}_2(\text{PEtPh}_2)_2]$: replacement of the PEt_3 ligand (electronic parameter $\chi = 5.6$, cone angle $\theta = 132^\circ$ [14]) by the poorer electron-donor PEtPh_2 ($\chi = 10.6$, $\theta = 140^\circ$ [14]) causes a significant increase in the K value so that such parameter can be determined from eqn. 9, and a

concomitant decrease of the corresponding k_{H} term of protonolysis from $(83 \pm 1) \times 10^{-3} \text{ M}^{-1} \text{ s}^{-1}$ [4] to $(1.6 \pm 0.1) \times 10^{-3} \text{ M}^{-1} \text{ s}^{-1}$ at 30 °C, due to a decreased electron density at the reaction site. Analogous and even more marked changes in K and k_{H} values are observed in the electrophilic cleavage of the Pt–Me bond when the aryl group Ar in *trans*-[PtMe(Ar)(PEt₃)₂] [5] is replaced by the more electronegative halide in *trans*-[PtXMe(PEt₃)₂] (X = Cl, Br).

References

- 1 M. D. Johnson, *Acc. Chem. Res.*, **11**, 57 (1978).
- 2 U. Belluco, R. A. Michelin, P. Uguagliati and B. Crociani, *J. Organomet. Chem.*, **250**, 565 (1983).
- 3 U. Belluco, U. Croatto, P. Uguagliati and R. Pietropaolo, *Inorg. Chem.*, **6**, 718 (1967).
- 4 R. Romeo, D. Minniti, S. Lanza, P. Uguagliati and U. Belluco, *Inorg. Chem.*, **17**, 2813 (1978).
- 5 R. Romeo, D. Minniti and S. Lanza, *J. Organomet. Chem.*, **165**, C36 (1979).
- 6 U. Belluco, M. Giustiniani and M. Graziani, *J. Am. Chem. Soc.*, **89**, 6494 (1967).
- 7 P. Uguagliati, R. A. Michelin, U. Belluco and R. Ros, *J. Organomet. Chem.*, **169**, 115 (1979).
- 8 J. K. Jawad, R. J. Puddephatt and M. A. Stalteri, *Inorg. Chem.*, **21**, 332 (1982).
- 9 J. Chatt and B. L. Shaw, *J. Chem. Soc.*, 705 and 4020 (1959).
- 10 C. Eaborn, K. J. Odell and A. Piccock, *J. Chem. Soc., Dalton Trans.*, 357 (1978).
- 11 P. Uguagliati, A. Benedetti, S. Enzo and L. Schiffini, *Comput. Chem.*, **8**, 161 (1984).
- 12 C. D. Falk and J. Halpern, *J. Am. Chem. Soc.*, **87**, 3523 (1965).
- 13 A. Tamaki and J. K. Kochi, *J. Chem. Soc., Dalton Trans.*, 2620 (1973).
- 14 C. A. Tolman, *Chem. Rev.*, **77**, 313 (1977).